SARS-CoV-2 Infection or COVID-19 mRNA Vaccination Elicit Similar Spike-Reactive Memory B Cell Responses in Naïve Individuals

Lingling Yao , Noémi Becza , Magdalena Tary-Lehmann , Greg A. Kirchenbaum , Paul V. Lehmann *

Posted Date: 24 July 2025

doi: 10.20944/preprints202507.1994.v1

Keywords: ELISPOT; FluoroSpot; immunological memory; humoral; Ig class; IgG subclass; plasma cell; immune monitoring

 doi:10.20944/preprints202507.1994.v1

Article

SARS-CoV-2 infection or COVID-19 mRNA vaccination elicit similar Spike-reactive memory B cell responses in naïve individuals

Lingling Yao [1], Noémi Becza [1], Magdalena Tary-Lehmann [2], Greg A. Kirchenbaum [1,†] and Paul V. Lehmann [1,*,†]

[1] Research and Development, Cellular Technology Ltd. (CTL), Shaker Heights, OH 44122, USA

[2] Contract Laboratory, Cellular Technology Ltd. (CTL), Shaker Heights, OH 44122, USA

* Correspondence: paul.lehmann@immunospot.com; Tel.: +1-(216)-791-5084

† These authors contributed equally to this work and share senior authorship.

Abstract

Background: The COVID-19 pandemic provided a unique opportunity to evaluate how the human immune system responded to a novel pathogen, and to determine whether immune responses initiated through natural infection differ from those elicited by vaccination against the same antigen. Here, we provide a comprehensive analysis of SARS-CoV-2 Spike (S-antigen)-reactive memory B cells (B_{mem}) elicited in previously immunologically naïve subjects following their first infection with the original Wuhan-Hu-1 (WH1)-like strain, or their initial COVD-19 mRNA prime-boost regimen encoding the same WH1-S-antigen. In particular, we tested the hypothesis that the primary encounter of SARS-CoV-2 S-antigen in lung mucosal tissues during infection vs. intramuscular COVID-19 mRNA injection would elicit different B_{mem} responses. **Methods:** Cryopreserved peripheral blood mononuclear cell (PBMC) samples collected following primary infection with the WH1 strain or completion of the initial prime-boost vaccination regimen were tested in ImmunoSpot® assays to assess the frequency, Ig class/subclass usage, and cross-reactivity of the S-antigen-reactive B_{mem} compartment; pre-pandemic blood draws served as naïve controls**. Results**: The B_{mem} repertoires generated post-infection vs. post-vaccination were found to be quite similar, but with some subtle differences. In both cases, the prevalent induction of IgG1-expressing B_{mem} in similar frequencies was seen, ~30% of which targeted the receptor binding domain (RBD) of the WH1-S-antigen. Also, the extent of cross-reactivity with the future Omicron (BA.1) RBD was found to be similar for both cohorts. However, IgA^+ B_{mem} were preferentially induced after infection, while $IgG4^+$ B_{mem} were detected only after vaccination. **Conclusions:** B_{mem} elicited in naïve human subjects following SARS-CoV-2 infection or after WH1-S-antigen encoding mRNA vaccination were only subtly different. Our findings serve to illustrate the usefulness and feasibility of performing comprehensive monitoring of antigen-specific B cell memory in larger cohorts using the ImmunoSpot® technique.

Keywords: ELISPOT; FluoroSpot; immunological memory; humoral; Ig class; IgG subclass; plasma cell; and immune monitoring

Introduction

Mucosal surfaces (e.g. respiratory-, gastro-intestinal-, and urogenital tracts) that segregate the outside world from the inside of the body are constantly exposed to environmental antigens. Such surfaces are continuously monitored for intrusion of foreign antigens by a specialized compartment of the immune system, the Mucosa-Associated Lymphoid Tissue (MALT) [1]. Bearing similar, yet distinct, structural organization as secondary lymphoid tissues (e.g. regional lymph nodes and the spleen), initiation of a B cell response in MALT preferentially leads to production of antigen-specific dimeric IgA that is transported across the epithelial layer via the polymeric immunoglobulin receptor

 doi:10.20944/preprints202507.1994.v1

(pIgR) into mucosal fluids and confers protection through hindering attachment of antigen(s) to epithelial cells [2]. Additionally, antigens encountered at the mucosa can also elicit IgG antibody responses that are readily detectable in plasma/serum [3–5]. In contrast to this natural route of infection, antigen exposure via a systemic route (e.g. intramuscular immunization) primarily elicits an IgG response. IgG can penetrate most tissues of the body where it serves to limit antigen dissemination through direct neutralization, facilitation of phagocytosis through generation of immune complexes, opsonization, activation of complement, or by mediating directed killing of antigen-expressing cells by natural killer cells through antibody-dependent cell-mediated cytotoxicity (ADCC) [6]. Notably, IgA is also present in plasma/serum, but exists predominantly as a monomer, and possesses similar effector functions as IgG such as antigen neutralization, complement fixation and the ability to interact with myeloid cells via binding with FcαRI [7–9].

Owing to alternative routes of entry and stimulatory context, mucosal and systemic antigen exposure can elicit different $CD4^+$ helper T cell responses. Whereas mucosal antigen exposure can induce tolerogenic responses, such as causing induction of nasal- [10–12] or oral tolerance [13], systemic encounter more commonly induces Th1 or Th2 type $CD4^+$ helper T cell responses that are dependent on the nature of "danger" signals associated with the antigen [14–17]. As the location of the antigen encounter (mucosal vs. systemic) and the specific cytokine milieu in the priming environment following natural infection with SARS-CoV-2 vs. COVID-19 mRNA vaccination differ fundamentally, we tested the hypothesis that the resulting B_{mem} directed against Spike (S-antigen) protein would also differ.

Depending on the type of $CD4^+$ T cell help provided during the primary immune response (guided by "danger" signals present during T cell priming/polarization), naïve B cells (that express IgM) undergo instructed Ig class switching to downstream heavy chain constant regions encoding IgA, IgE, or IgG [18]. Notably, in humans there are four IgG subclasses (IgG1/IgG2/IgG3/IgG4) that each possess distinct effector functions owing to their variable engagement with FcγR expressed by cells of the innate immune system [19]. Importantly, Ig class switching is an irreversible process that leads to permanent excision of all upstream IgH gene elements from the loci [18]. Thus, while naïve B cells are uncommitted prior to antigen encounter, the resulting effector- and memory B cell (B_{mem}) progeny are biased in their Ig expression/secretion; although subsequent switching to downstream Ig class/subclass encoding genes is still possible in some instances [20].

To unambiguously address our hypothesis that S-antigen-reactive B_{mem} will differ after primary SARS-CoV-2 infection vs. COVID-19 mRNA vaccination, and in order to cirumvent additional complexities arising as a consequence of subsequent S-antigen exposures (e.g. booster vaccination and/or breakthrough infections), we restricted our study to individuals for whom we could verify that the induction of S-antigen-reactive B_{mem} occurred either during the first wave of the COVID epidemic in subjects with PCR-verified infection, or, concerning the vaccinated cohort, to individuals who were immunized shortly after the vaccine become widely available (April/May 2021), before widespread infections with SARS-CoV-2 Omicron variants occurred [21].

There are numerous publications describing serum antibodies after SARS-CoV-2 infection or COVID-19 mRNA vaccination (reviewed in [22,23]). For reasons anchored in basic B cell biology, however, serum antibodies do not accurately reflect on B_{mem} generation. This is because the emergence of the ensuing plasma cell progeny (the source of plasma/serum antibodies) and B_{mem} follow distinct instructed differentiation pathways [24] (Supplemental Figure S1). When naïve B cells first encounter their cognate antigen in secondary lymphoid tissues (e.g. draining lymph nodes) they become activated and proliferate (clonal expansion). Following interactions with follicular T helper cells some of these activated B cells migrate into germinal centers where they undergo further rounds of cell division. Additionally, Ig class switching and acquisition of somatic hypermutations in the variable (antigen binding) domains of their B cell receptor (BCR) also occurs. As a consequence of the latter, the daughter cells of a single B cell can express a BCR with either a higher, lower, or (in spite of somatic mutations) an unaltered affinity for the antigen. Of these mutated subclones, those that have an increased affinity for the antigen will be positively selected for differentiation into the plasma

 doi:10.20944/preprints202507.1994.v1

cell lineage, while subclones not meeting the high affinity criterion will instead preferentially differentiate into B_{mem} [24,25]. Whereas the affinity-based selection for plasma cell differentiation serves to improve the efficacy of the ensuing antibody response against the invading (homotypic) virus, the broadened specificity of B_{mem} arising as a consequence of sustained germinal center reactions also increases the likelihood that B_{mem} with reactivity against future antigenic variants are also generated [26]. Even if the frequency of B_{mem} with specificity for an emerging variant strain is low amongst the memory repertoire, their frequency is still increased relative to naïve B cells, i.e., they exist in a clonally expanded state, are already class-switched, and hence can generate faster anamnestic (secondary-type) antibody responses following encounter with antigenic variants [25]. Consequently, to achieve a holistic understanding of B cell-mediated immune protection and specifically the ability of a pre-immune host to recognize future antigenic variants, studies of plasma/serum antibodies alone cannot substitute for studies of B_{mem} themselves [27].

While studies of B_{mem} are necessary to achieve a better understanding of B cell-mediated immunity, there remains a paucity of such. The reason is that such studies, unlike antibody measurements, have been challenging. Technical difficulties to overcome include the low frequency of B cells specific for any given antigen even when the B cells exist in a clonally expanded state within all PBMC. Classic approaches like growing individual clones/hybrids are limited by their labor requirements and low throughput [28]. Single cell paired *IgH*/*IgL* sequencing is also a promising novel approach, but only provides indirect data on the frequency and specificity of B_{mem} unless the antibodies are recombinantly expressed and subsequently tested for their actual binding properties as only a fraction of the B cells identified may actually be antigen specific [29]– an effort again too demanding for comprehensive immune monitoring in sizeable donor cohorts. Staining antigen-specific B cells with fluorophore-labelled antigen probes followed by flow cytometric analysis is also a promising approach; however, it is frequently hampered by the complexities of achieving specific probe staining and the detection limit for cells that occur at very low frequencies [29]. Finally, ELISPOT/FluoroSpot (collectively called ImmunoSpot®) in theory bypasses the limitations of the above tests. However, in its original implementation (Supplemental Figure S2A), this technique often fails to detect antigen-specific B_{mem} following their differentiation into antibody-secreting cells (ASCs) owing to insufficient antigen coating of the assay membrane [30]. Realizing that many antigens, including the receptor binding domain (RBD) of SARS-CoV-2 S-antigen or nucleocapsid (NCAP), do not bind in sufficient density when coated directly onto the plates and thus cannot reveal the secretory footprints originating from individual antigen-specific B cells, we introduced an affinity coating strategy (Supplemental Figure S2B) that has made ImmunoSpot®-based detection of B_{mem} universally feasible [30]. Taking advantage of this new development, along with additional refinements in the assay procedure itself [31–33], here we report an in-depth analysis of B_{mem} repertoires generated following recovery from SARS-CoV-2 infection or after prime-boost COVID-19 mRNA vaccination of previously immunologically naïve subjects.

2. Materials and Methods

2.1. Human Subjects

Peripheral blood mononuclear cell (PBMC) samples originating from three defined cohorts were characterized in this study. The first cohort, collected prior to November 1, 2019, constituted the pre-COVID samples. The second cohort, collected from convalescent human subjects following verification of SARS-CoV-2 infection by polymerase chain reaction (PCR) testing, constituted the post-infection cohort. Samples from both the pre-COVID and post-infection cohorts were collected at FDA-registered collection centers and were obtained from IRB-consented healthy human donors by leukapheresis and then were sold to CTL identifying donors by code only while concealing the subjects' identities. PBMC were cryopreserved according to previously described protocols [33]. Additionally, blood samples from a third cohort were collected internally at CTL under an Advarra approved IRB #Pro00043178 (CTL contract laboratory study number GL20-16 entitled COVID-19

 doi:10.20944/preprints202507.1994.v1

Immune Response Evaluation) and PBMC were isolated and cryopreserved according to previously described protocols [33]. All PBMC samples were stored in liquid nitrogen until testing. Details of all human donors included in this manuscript, including demographics, collection dates, and duration since SARS-CoV-2 infection or COVID-19 mRNA vaccination are provided in Supplemental Table S1.

2.2. Polyclonal B cell Stimulation

Detailed methods of thawing, washing and counting of PBMC have been previously described [33]. Cells were seeded into polyclonal B cell stimulation cultures within 2 h of thawing. Freshly thawed PBMC samples were resuspended in complete medium containing RPMI 1640 (Alkali Scientific, Fort Lauderdale, FL) supplemented with 10% fetal bovine serum (Gemini Bioproducts, West Sacramento, CA), 100 U/mL penicillin, 100 U/mL streptomycin, 2 mM L-Glutamine, 1 mM sodium pyruvate, 8 mM HEPES (all from Life Technologies, Grand Island, NY) and 50 µM β-mercaptoethanol (Sigma-Aldrich, St. Louis, MO). PBMC were then stimulated with Human B-Poly-S (CTL) containing TLR7/8 agonist R848 and recombinant human IL-2 [34] at 0.5-2 x 10^6 cells/mL in 25 cm^2 or 75 cm^2 tissue culture flasks (Corning, Sigma-Aldrich) and incubated at 37°C, 5% CO_2 for 5 days to promote terminal differentiation of resting B cells into antibody-secreting cells (ASCs) prior to evaluation in ImmunoSpot® assays.

2.3. Recombinant Proteins

Recombinant full-length SARS-CoV-2 Spike (S-antigen) protein representing the ancestral Wuhan-Hu-1 strain [35], denoted as WH1-S (FL), or a truncated version encoding only the receptor binding domain (RBD) [36], denoted as WH1-S (RBD), were acquired from the Center for Vaccines and Immunology (CVI) (University of Georgia (UGA), Athens, GA, USA). RBD protein representing the Omicron variant (BA.1), denoted as BA.1-S (RBD), was purchased from Creative Biomart (Shirley, NY, USA). Recombinant SARS-CoV-2 Nucleocapsid (NCAP) protein was purchased from the Wuhu Interferon Biological Products Industry Research Institute (Wuhu, Anhui Province, China). Importantly, all recombinant proteins used in this study possessed a genetically-encoded His affinity tag.

2.4. B cell ImmunoSpot® Assays

2.4.1. Multiplexed antigen-specific FluoroSpot assays with affinity capture coating

For detection of antigen-specific ASCs in multiplexed FluoroSpot assays using the affinity capture coating method [30], low autofluorescence FluoroSpot assay wells were first pre-conditioned with 70% (*v*/*v*) EtOH (15 µL/well) followed by two washes with phosphate-buffered saline (PBS) (150 µL/well) prior to coating with purified anti-His antibody at 10 µg/mL in Diluent A (provided in CTL's affinity coating kits) overnight at 4°C. The following day, FluoroSpot assay plates were washed once with 150 µL (PBS and then coated overnight at 4°C with His-tag labeled recombinant WH1-S (FL) or WH1-NCAP protein at 10 µg/mL in Diluent A. Prior to use, assay plates were washed once with 150 µL PBS, and then blocked with complete medium for 1 h at room temperature (RT). Immediately prior to plating of cells, assay plates were decanted and 100 µL pre-warmed complete medium was added to each well.

PBMC were collected after 5 days of polyclonal stimulation and washed twice with PBS prior to counting using CTL's Live/Dead Cell Counting Suite on an ImmunoSpot® S6 Flex Analyzer (CTL). Cell pellets were resuspended at 5 × 10^6 live cells/mL in complete medium and used immediately in ImmunoSpot® assays. To increase the WH1-S (FL) assay's sentivity for detecting rare antigen-reactive ASCs, pre-COVID era samples were tested in three replicate wells seeded with 5 x 10^5 polyclonally stimulated PBMC. Alternatively, post-infection or post-vaccination samples were tested using a singlet two-fold serial dilution approach starting at 5 x 10^5 live cells per well. To avoid damage to the assay membrane, PBMC were serially diluted in round bottom 96-well tissue culture plates (Corning,

 doi:10.20944/preprints202507.1994.v1

Sigma-Aldrich) and then subsequently transferred into assay plates, as previously described [33]. Samples from the post-infection and post-vaccination cohorts were additionally tested for WH1-S (FL)-reactive ASCs in a two-fold dilution series starting at 5 x 10^4 PBMC per well to improve the accuracy of frequency determinations for samples with an abundance of spot-forming units (SFUs). For WH1-NCAP ImmunosSpot® assays, all samples were tested in three replicate wells seeded with 5 x 10^5 polyclonally stimulated PBMC to improve the assay's limit of detection. Following plating of PBMC, assay plates were incubated for 16 h at 37°C, 5% CO_2. Plate-bound SFUs, each representing the secretory footprint of a single ASC, were visualized using either IgA, IgE-, IgG- and IgM-specific detection reagents or IgG1-, IgG2-, IgG3-, and IgG4-specific detection reagents, according to the manufacturer's instructions (CTL).

2.4.2. Multiplexed pan Ig class and subclass detection

To verify ASC functionality in the polyclonally stimulated PBMC samples, pan Ig class (IgA/IgE/IgG/IgM) and IgG subclass (IgG1/IgG2/IgG3/IgG4) ImmunoSpot® assays were set up in parallel with the antigen-specific assays detailed above. For detecting all ASCs, irrespective of their antigen specificity, cell suspensions were serially diluted two-fold in singlets, starting at 2 × 10^5 or 2 × 10^4 PBMC per well in round bottom 96-well tissue culture plates and subsequently transferred into low autofluorescence FluoroSpot assay plates that were coated overnight at 4°C (following pre-wetting with 70% (*v*/*v*) EtOH as described above) with anti-κ/λ capture antibody contained in the human IgA/IgE/IgG/IgM Four-Color ImmunoSpot® kit or IgG1/IgG2/IgG3/IgG4 Four-Color ImmunoSpot® kit (from CTL). FluoroSpot plates were then washed with PBS and blocked with complete medium as described above. Following plating of PBMC, assay plates were incubated for 16 h at 37°C, 5% CO_2. Plate-bound SFUs, each representing the secretory footprint of a single ASC irrespective of antigen specificity, were subsequently visualized using either IgA, IgE-, IgG- and IgM-specific detection reagents or IgG1-, IgG2-, IgG3-, and IgG4-specific detection reagents, according to the manufacturer's instructions (CTL).

2.4.3. Single-color inverted FluoroSpot assays for detection of SARS-CoV-2 S-reactive IgG^+ ASC

To further restrict the reactivity of S-antigen-reactive ASCs to the receptor binding domain (RBD), polyclonally stimulated PBMC samples from the post-infection and post-vaccination cohorts were also tested in IgG-specific inverted ImmunoSpot® assays using His affinity tagged WH1-S (FL) or RBD proteins representing the WH1 or Omicron variant BA.1 strains as detection probes. In brief, low autofluorescence FluoroSpot assay plates were coated overnight at 4°C (following pre-wetting with 70% (*v*/*v*) EtOH) with anti-human IgG Fc capture antibody at 15 µg/mL in Diluent A (provided in CTL's inverted ImmunoSpot® kits). FluoroSpot plates were then washed with PBS and blocked with complete medium as described above. Polyclonally stimulated PBMC samples from the post-infection and post-vaccination cohorts were then plated in eight replicate wells at donor-specific inputs (referred to as the "Goldilocks cell input") previously determined to yield ~50 WH1-S (FL)-reactive IgG^+ SFUs in assays utilizing the affinity capture coating methodology. Following plating of PBMC, assay plates were incubated for 16 h at 37°C, 5% CO_2. After washing, His-tagged WH1-S (FL) at 2 µg/mL, WH1-S (RBD) at 100 ng/mL, or BA.1-S (RBD) at 100 ng/mL in Diluent B (provided in CTL's inverted ImmunoSpot® kits) was added into the designated wells, respectively, and incubated for 2 h at RT. After decanting and washing, anti-His detection antibody conjugated with Alexa Fluor® 488 (provided in CTL's His inverted ImmunoSpot® kit) was added to the designated wells, and incubated for 1 h at RT to visualize individual S-antigen-reactive SFUs.

2.4.4. FluoroSpot Image Acquisition and SFU Counting

FluoroSpot plates were air-dried prior to scanning on an ImmunoSpot® Ultimate S6 Analyzer using the Fluoro-X suite of ImmunoSpot® software (Version 7.0.28) (CTL). Quantification of SFUs in assay wells was performed using ImmunoSpot® Studio.SC software (Version 1.7.28.0) and B cell

 doi:10.20944/preprints202507.1994.v1

IntelliCount™ algorithms [37] or the Basic Count mode. Individual well images were quality controlled to remove artifacts and improve accuracy of counts as needed. Only SFU counts within the linear titration range of the ImmunoSpot® assay, or SFU counts from the highest cell input tested, were considered for frequency calculations and were subsequently used to extrapolate SFU counts to a fixed input of 10^6 PBMC. As ImmunoSpot® Multi-color B cell kits, analyzers, and software proprietary to CTL were used in this study, we refer to the collective methodology as ImmunoSpot®.

2.5. Statistical Methods

Statistically significant differences in the frequency of WH1-S (FL)- and WH1-NCAP-specific ASCs were determined using unpaired t-tests (GraphPad Prism 10 Version 10.4.0, San Diego, CA, USA) and are denoted in the corresponding figure legends. To determine the relative frequency of WH1-S (FL)-reactive IgG^+ ASCs that recognized epitopes in the RBD region of the WH1 or BA.1 variant strains, the cumulative SFU count from replicate wells probed with the WH1-S (FL) protein was designated as the 100% value. The cumulative SFU counts from replicate wells probed with either the WH1-S (RBD) or BA.1-S (RBD) proteins were then divided by this SFU value (corresponding to 100% of the WH1-S (FL)-reactive response at the donor-specific PBMC input) and are expressed as a percentage.

3. Results and Discussion

3.1. Establishing the frequency of SARS-CoV-2 Spike (S)- and Nucleocapsid (NCAP)-reactive IgG^+ B_{mem} in defined PBMC cohorts

Having developed an affinity coating strategy (Supplementary Figure S2B) that enabled detection of secretory footprints from SARS-CoV-2 S-antigen- or NCAP-reactive IgG^+ B_{mem} [30], here we sought to more stringently define the characteristics of these antigen-specific cells. To this end, and accounting for possible chance cross-reactivity with common cold coronaviruses (CCC) that were in circulation prior to the emergence of SARS-CoV-2 [38], ImmunoSpot® assays enabling visualization of secretory footprints generated by IgG-secreting B cells with reactivity to a full-length S-antigen representing the ancestral Wuhan-Hu-1 strain, denoted as WH1-S (FL), or WH1- NCAP protein were performed using polyclonally stimulated PBMC originating from three defined cohorts (pre-COVID, post-infection or post-vaccination; detailed below). Importantly, because in previous studies we observed that frequencies of WH1-S-reactive IgG^+ B_{mem} in convalescent subjects were present over a broad frequency range [39], PBMC from the post-infection or post-vaccination cohorts were tested for reactivity against the WH1-S (FL) protein using a single well serial dilution strategy starting at 5 x 10^5 PBMC per well [32]. Alternatively, a fixed cell input of 5 x 10^5 PBMC in three replicate wells was used for testing the pre-COVID cohort for WH1-S (FL)-reactive ASC to improve the limit of detection for rare ASCs. Lastly, since frequencies of WH1-NCAP-reactive ASCs tended to be lower than those specific for the S-antigen, PBMC samples from all cohorts were tested at a fixed input of 5 x 10^5 PBMC in three replicate wells.

The first PBMC cohort detailed in this communication, constituting pre-COVID era blood draws (cryopreserved before November 1, 2019) might exhibit chance cross-reactivity with third-party antigens, such as those corresponding to antigens expressed by CCC, but importantly would not have been exposed to SARS-CoV-2 itself owing to their date of collection prior to the first confirmed SARS-CoV-2 infection in the United States [40]. The second PBMC cohort originated from convalescent donors who recovered from PCR-verified SARS-CoV-2 infections in the early months of 2020 at the onset of the COVID-19 epidemic and before vaccines became widely available. These individuals would be expected to have developed B_{mem} to both WH1-S (FL) and WH1-NCAP proteins. The third PBMC cohort consisted of those who were prime-boost immunized with COVID-19 mRNA vaccine (encoding the WH1-S protein) soon after it became available in April/May 2021, and before widespread SARS-CoV-2 infections with the Omicron variant strains occurred [21]. In these subjects we expected to detect WH1-S (FL), but not WH1-NCAP-reactive IgG^+ B_{mem} (unless some of these

 doi:10.20944/preprints202507.1994.v1

individuals had subclinical SARS-CoV-2 infection, in addition, for which we controlled through testing the polyclonally stimulated PBMC samples for IgG⁺ ASC reactivity against the WH1-NCAP protein).

For IgG measurements such ImmunoSpot® assays revealed exquisite specificity (Figure 1A,B): none of the pre-COVID era PBMC harbored appreciable WH1-S (FL)- and WH1-NCAP-reactive IgG-producing B_{mem} -- thus no false positives were seen. These data also suggest that prior CCC infection(s), had they occurred in our pre-COVID era donors, failed to elicit a sizeable population of IgG⁺ B_{mem} with cross-reactivity for the WH1-S (FL) antigen. In contrast, all PBMC samples from the post-infection and post-vaccination cohorts contained WH1-S (FL)-reactive IgG⁺ B_{mem}, and notably, the frequencies of such cells were similar in the two cohorts at the time of testing (3 -7 months after induction of the B cell responses). As expected, NCAP-reactive IgG⁺ B_{mem} were detected in all of the previously infected donors, albeit at much lower frequencies than were detected for WH1-S (FL). However, NCAP-reactive IgG⁺ B_{mem} were absent in tests utilizing PBMC from the pre-COVID or post-vaccination cohorts. These data support the notion that the post-vaccination cohort had neither been infected with SARS-CoV-2 prior to their vaccination, nor during the elapsed time between their vaccination and the blood collections. Therefore, as was the intent of this study, the primary induction of WH1-S (FL)-reactive IgG⁺ B_{mem} was what was indeed being monitored in the post-infection and post-vaccination cohorts.

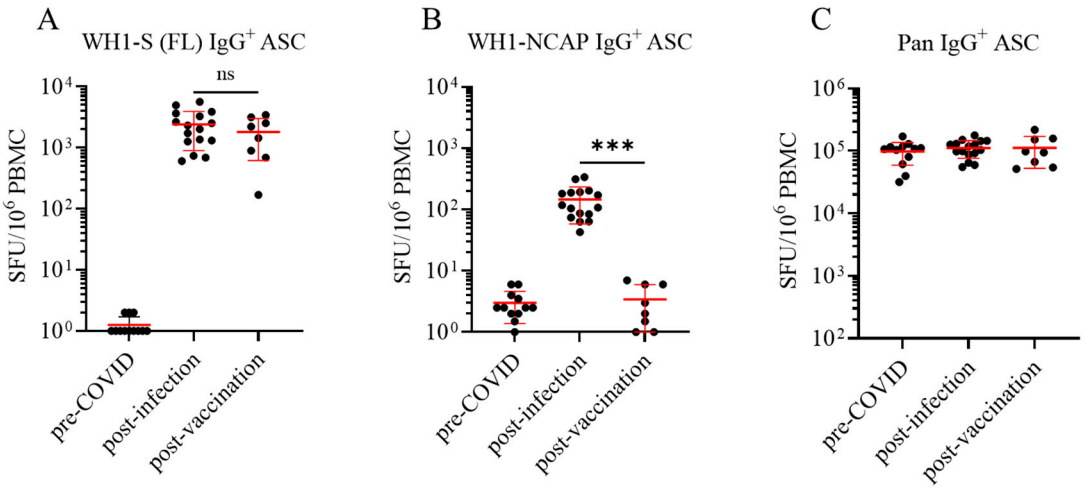

Figure 1. Frequency of WH1-FL S- and NCAP-specific IgG⁺ ASC in defined cohorts of cryopreserved PBMC. Peripheral blood mononuclear cells (PBMC) collected from SARS-CoV-2 infected (n=16, denoted as post-infection cohort) and COVID-19 mRNA vaccinated (n=8, denoted as post-vaccination cohort) or pre-COVID era controls (n=12) were subjected to in vitro polyclonal stimulation with Human B-Poly-S (R848+rIL-2) to convert resting B cells into antibody-secreting cells (ASCs) for subsequent evaluation in multiplexed B cell FluoroSpot assays (refer to Sections 2.2 and 2.4) A) Frequencies of IgG⁺ ASCs specific for a full-length SARS-CoV-2 Spike protein representing the Wuhan-Hu-1 strain, denoted as WH1-S (FL), were calculated using spot-forming unit (SFU) counts occurring in the linear range and extrapolated to SFU per 10^6 PBMC. Each data point denotes an individual donor in the respective cohorts and the mean ± SD for each cohort is shown in red. Donors in the pre-COVID cohort lacking detectable WH1-S (FL)-reactive IgG⁺ ASCs were assigned a value of 1 SFU per 10^6 PBMC for graphing purposes. Statistical significance (***$p<0.001$) of the difference between pre-COVID era and post-infection or post-vaccinated PBMC samples was determined using an unpaired t-test; note, the frequencies of WH1-S (FL)-specific IgG⁺ ASCs in the infected and vaccinated cohorts were not significantly different ($p=0.34$). B) Frequencies of IgG⁺ ASCs specific for the SARS-CoV-2 WH1 Nucleocapsid protein, denoted as WH1-NCAP, are expressed as SFU per 10^6 PBMC. Statistical significance (***$p<0.001$) of the difference between infected and vaccinated donor cohorts was determined using an unpaired t-test. C) Frequencies of pan (total) IgG⁺ ASCs,

 doi:10.20944/preprints202507.1994.v1

detected irrespective of antigen specificity (refer to Supplemental Figure S2C), are expressed as SFU per 10^6 PBMC.

Notably, measurement of B_{mem} secreting antibody of undefined specificity in pan IgG assays (Figure 1C, please refer to Supplementary Figure S2C for the assay principle) performed in parallel confirmed that pre-COVID era PBMC samples were indeed functional and hence capable of successful differentiation into IgG^+ ASCs following polyclonal stimulation. Therefore, the failure to detect WH1-S (FL)- or WH1-NCAP-reactive IgG^+ B_{mem} in pre-COVID era samples was not a consequence of their impaired IgG^+ ASC activity. Moreover, pre-COVID era samples exhibited similar frequencies of B_{mem}-derived IgG^+ ASCs with reactivity for alternative antigens representing seasonal influenza or Epstein-Barr virus [39]. Owing to the considerable inter-individual variation in the frequency of pan IgG^+ ASCs following polyclonal stimulation of PBMC, we also present the frequency of WH1-S (FL)-reactive and WH1-NCAP-reactive IgG^+ B_{mem}-derived ASCs amongst all IgG^+ ASCs (Supplementary Figure S3).

3.2. Defining Ig classes of B_{mem} elicited by natural infection vs. vaccination

Immunoglobulins (Ig) occur in the classes IgM, IgD (expressed by naïve B cells, primarily), as well as IgG, IgA and IgE, that are expressed on the surface of resting B cells constituting their BCR, or are secreted following their differentiation into an ASC. Surface expression or secretion of a class-switched Ig (IgG, IgA or IgE) is an indicator that a B cell has previously participated in a classical T cell-dependent immune response. As the different classes of antibodies play fundamentally different roles in host defense, we compared Ig class utilization of the WH1-S (FL)-reactive B_{mem} generated following SARS-CoV-2 infection or COVID-19 mRNA vaccination, along with PBMC samples from the pre-COVID era cohort as controls. Four-color multiplexed ImunoSpot® assays were performed to enable simultaneous detection of IgM-, IgG-, IgA- or IgE-secreting cells (note that these assays offer similar sensitivity as single-color ELISPOT tests [32,33]). Using such four-color assays, we characterized the WH1-S (FL)-reactive B cell repertoires in the three cohorts. In contrast to the clear-cut IgG results shown in Figure 1, the frequency of WH1-S (FL)-reactive IgM^+ ASCs was similar in all three cohorts (Figure 2A), i.e., such cells were detected in the pre-COVID era donors as well, a finding suggesting that these IgM^+ ASCs are not derived from antigen-experienced B_{mem}, but instead likely reflect the presence of low-affinity, broadly cross-reactive naïve B cells that differentiated into ASCs following polyclonal stimulation. The presence of IgM^+ WH1-S (FL) reactive ASCs in pre-COVID donors, as well as the ocurrance of pan IgM^+ ASCs in similar numbers in all three cohorts (Figure 2B) provided further evidence for the unimpaired functionality of the pre-COVID PBMC samples.

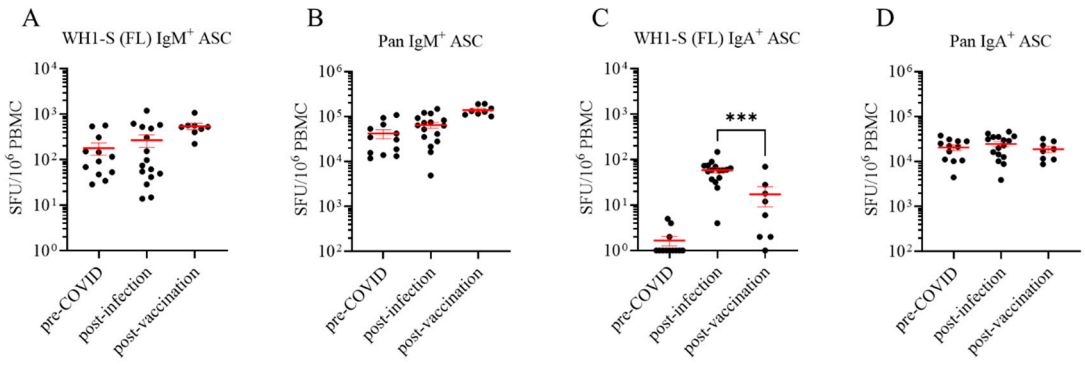

Figure 2. Assessment of WH1-S (FL)-reactive IgM^+ and IgA^+ ASCs in defined cohorts of cryopreserved PBMC. Peripheral blood mononuclear cells (PBMC) collected from SARS-CoV-2 infected (n=16), COVID-19 mRNA vaccinated (n=8) or pre-COVID era controls (n=12) were evaluated for reactivity against the WH1-S (FL) protein in multiplexed B cell FluoroSpot assays as described in Figure 1 (refer to Section 2.4 for additional details). Frequencies of IgM^+ (panel A) and IgA^+ (panel C) ASCs reactive to WH1-S (FL) are expressed as SFU per 10^6

 doi:10.20944/preprints202507.1994.v1

PBMC. Donors lacking detectable WH1-S (FL)-reactive IgA$^+$ ASCs were assigned a value of 1 SFU per 10^6 PBMC for graphing purposes. Frequencies of pan (total) IgM$^+$ (panel B) and IgA$^+$ (panel D) ASCs, irrespective of antigen specificity, are expressed per 10^6 PBMC. Note: results for IgE are not shown since they were negative; including the lack of pan IgE$^+$ ASC detection.

WH1-S (FL)-reactive IgA$^+$ ASCs (whose mere presence, like for IgG, and unlike for IgM, implies that such cells have undergone antigen-driven T cell-dependent Ig class switching) were readily detected in 15 of 16 samples from the post-infection cohort but only in 4 of 8 samples from the post-vaccination cohort and at significantly lower frequencies (Figure 2C). The similar frequencies of pan IgA$^+$ ASCs between the three donor cohorts (Figure 2D) further confirmed the functionality of the PBMC samples cannot account for the observed differences in WH1-S (FL)-reactive IgA$^+$ B_{mem} frequencies. Overall, frequencies of WH1-S (FL)-reactive IgA$^+$ B_{mem}-derived ASCs were considerably lower than the frequency of WH1-S (FL)-reactive IgG$^+$ B_{mem}-derived ASCs in both the convalescent and vaccinated cohorts. These data are also in line with the notion that SARS-CoV-2 infection of the upper respiratory tract mucosa and lung elicited a more robust induction of IgA$^+$ B_{mem} circulating in peripheral blood compared to intramuscular injection of the COVID-19 mRNA vaccine. We contend that analagous B cell ImmunoSpot® assays as described herein would be ideally-suited to comprehensively address the question of whether SARS-CoV-2 infection or prime-boost COVID-19 mRNA vaccination were equally capable of increasing the frequency of WH1-S (FL)-reactive IgA$^+$ or IgG$^+$ B_{mem} residing in draining lymph nodes, bronchus-associated lymphoid tissue (BALT), or the lung, but this could not be tested here.

Lastly, owing to the inclusion of IgE-specific detection reagents in the multiplexed B cell ImmunoSpot® assays, we can also report the failure to detect WH1-S (FL)-reactive IgE$^+$ ASC in any of the samples. Related to this, pan IgE$^+$ ASCs irrespective of antigen specificity were not detected either, consistent with the notion that circulating IgE$^+$ B_{mem} may not exist (or possibly, the generation of IgE$^+$ ASCs requires de novo class switching [20]). Consistent with this notion, we also observed that polyclonal stimulation of B cells in vitro under conditions that mimic T cell help (in the presence of agonistic anti-CD40 antibody plus IL-4 and IL-21) induced IgE$^+$ ASCs that were clearly detectable at single cell resolution using an equivalent ImmunoSpot® detection system [33]. In aggregate, these observations indicate that had pan IgE$^+$ ASCs been present in our polyclonally stimulated PBMC samples at frequencies exceeding the lower detection limit of the assay as performed, i.e., 1 in 2 x 10^5 PBMC, they would have been detected.

3.3. Dissecting IgG subclass utilization of WH1-S (FL)-reactive B_{mem} in infected or vaccinated subjects

IgG antibodies can be segregated into 4 subclasses, whose expression also depends on Ig class switching. Importantly, Ig expression is restricted through the process of allelelic exclusion, i.e., an individual B cell can express only one Ig class/subclass [41]. The four IgG subclasses trigger distinct engagement of innate immune reactions [19]. Namely, IgG1 and IgG3 excel in complement fixation and the induction of Fc-receptor-induced phagocytosis and ADCC. In contrast, IgG2 exhibits reduced affinity for FcγRs, particularly FcγRIIIb, and is less effective at triggering ADCC. However, under conditions of high antigen density, IgG2 is still capable of activating the complement cascade. Lastly, IgG4 possesses a reduced affinity for FcγR and does not efficiently trigger classical extra-neutralizing effector functions. Instead, IgG4 may possess anti-inflammatory properties through its ability to compete with other IgG subclasses for antigen binding. Notably, IgG4 can undergo Fab-arm exchange which renders it functionally monovalent [42]. Therefore, assessing the IgG subclass(es) expressed by WH1-S (FL)-reactive B_{mem} that were generated following SARS-CoV-2 infection vs. COVID-19 mRNA vaccination would unveil critical information regarding the type of protective immunity elicited by each.

To this end, we performed multiplexed ImmunoSpot® assays unambiguously detecting all four IgG subclasses: examples of representative wells are shown in Figure 3. As noted above, we had previously established that such four-color assays facilitated detection of secretory footprints with

 doi:10.20944/preprints202507.1994.v1

equal sensitivity to that of single-color ELISPOT measurements [32,33]. Consequently, parallel assessment of IgG subclass usage was enabled without increasing the amount of cell material required. Both the post-infection and post-vaccination cohorts displayed clearly elevated frequencies of WH1-S (FL)-reactive IgG1$^+$ ASCs (Figure 4A) at similar frequencies. Also, both donor cohorts possessed detectable WH1-S (FL)-reactive IgG3$^+$ ASCs, albeit at much lower frequencies than IgG1$^+$ ASCs. However, WH1-S (FL)-reactive IgG2$^+$ ASCs were essentially undetectable in both the post-infection and post-vaccination samples despite verification of IgG2$^+$ ASC activity when measured irrespective of their antigen specificity (Figure 4B). Lastly, while the frequencies of pan IgG4$^+$ ASCs were similar in both cohorts (Figure 4B), WH1-S (FL)-reactive IgG4$^+$ ASCs were significantly increased in the post-vaccination cohort only (Figure 4A).

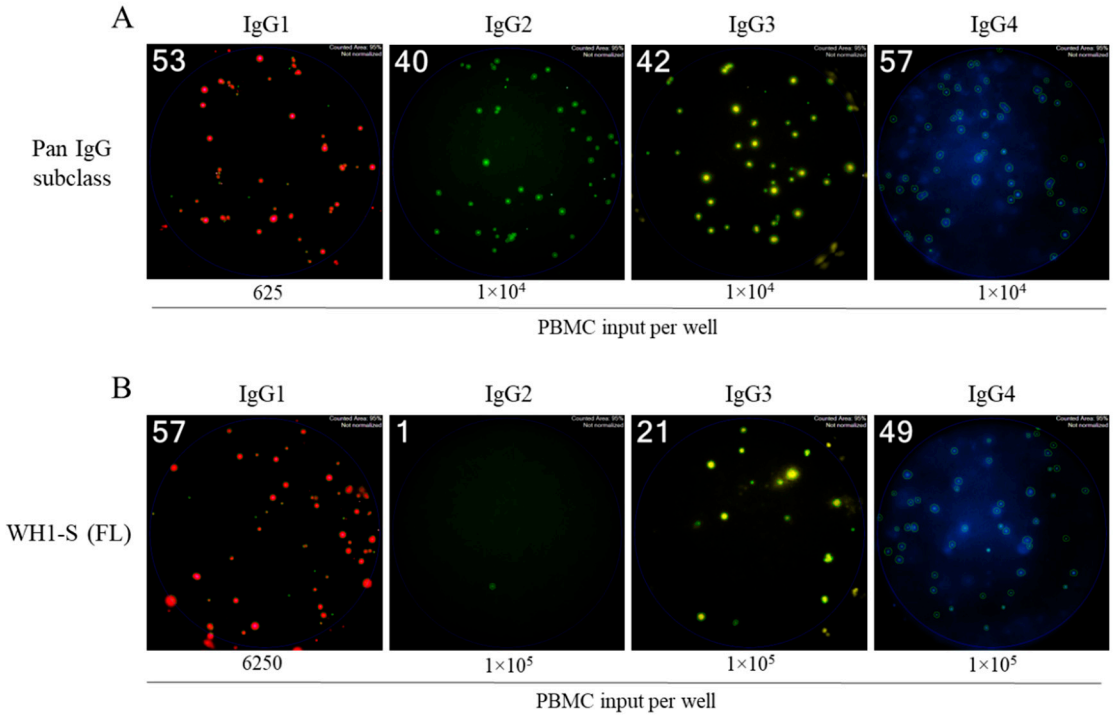

Figure 3. Four-color ImmunoSpot® assays enable parallel detection of IgG subclass usage. Representative well images from four-color multiplexed FluoroSpot assays enabling detection of "pan" antibody-secreting cells (ASCs) irrespective of their antigen specificity (panel A) or those secreting WH1-S (FL)-specific IgG (panel B). Cell inputs are specified below the corresponding images, which were contrast enhanced to aid visualization.

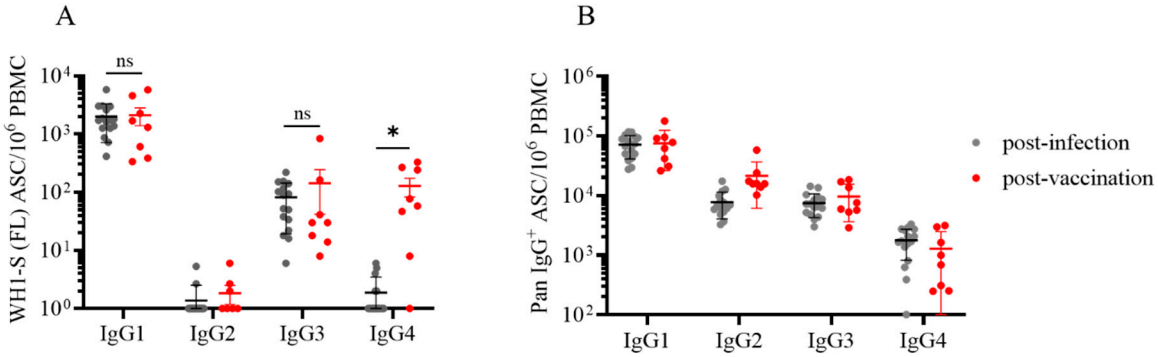

Figure 4. Evaluation of WH1-S (FL)-specific ASC IgG subclass usage in SARS-CoV-2-infected or COVID-19 mRNA-vaccinated donors. Peripheral blood mononuclear cells (PBMC) collected from SARS-CoV-2 infected (n=16) or COVID-19 mRNA vaccinated (n=8) donors were evaluated for reactivity against the WH1-S (FL)

 doi:10.20944/preprints202507.1994.v1

protein in multiplexed B cell FluoroSpot assays as described in Figure 1 (refer to Section 2.4 for additional details). A) Frequency of WH1-S (FL)-specific ASCs producing IgG1, IgG2, IgG3 or IgG4 are expressed as SFU per 10^6 PBMC. Frequencies of WH1-S (FL)-specific $IgG1^+$ or $IgG3^+$ ASCs in the infected or vaccinated donor cohorts were not significantly different, whereas the frequency of WH1-S (FL)-specific $IgG4^+$ ASCs was significantly increased (*$p<0.05$) in the vaccinated donor cohort by unpaired t-tests. B) Frequencies of pan (total) ASCs, irrespective of antigen specificity, producing IgG1, IgG2, IgG3 or IgG4 are expressed as SFU per 10^6 PBMC. Notably, the apparent absence of WH1-S (FL)-specific $IgG2^+$ ASCs was not attributable to impaired detection since pan $IgG2^+$ ASCs were present in all samples (see also Figure 3A).

Recently, increased attention has been focused on the emergence of IgG4 antibodies following repeated COVID-19 mRNA vaccinations [43]. While addressing the consequences of chronic antigen exposure is beyond the scope of this communication, we believe the observation that the post-vaccination cohort possessed an increased frequency of WH1-S (FL)-reactive $IgG4^+$ B_{mem}-derived ASCs after only the initial prime-boost vaccination regimen is noteworthy. In ongoing work we also identified several individuals exhibiting an increased frequency of WH1-S (FL)-reactive $IgG4^+$ ASCs after receiving multiple COVID-19 mRNA vaccinations (Kirchenbaum, work in progress). Shifting of the IgG subclass usage directed against the SARS-CoV-2 S-antigen is likely to have biological consequences since IgG4 binds FcγR with reduced affinity compared to IgG1 or IgG3, and consequently IgG4 is less efficient at mediating FcγR-dependent effector mechanisms [44,45]. In support of this notion, elevated titers of S-antigen binding IgG4 was associated with an increased risk for breakthrough infection [46].

We include Supplementary Figure S4 to better illustrate – by showing data on a linear scale -- how variable the frequencies of WH1-S (FL)-reactive ASCs producing different Ig classes or IgG subclasses are; four representative donors in the post-infection or post-vaccination study cohorts are shown. The data also reiterate the requirement to perform serial dilutions when performing frequency measurements for the individual Ig classes and subclasses.

3.4. Characterization of RBD-reactive B_{mem} induced in infected or vaccinated subjects

While antibodies targeting any exposed region of a viral antigen can contribute to host defense [47,48], antibodies that are endowed with neutralizing activity are of particular significance [49]. In the most simplified scenario, a virus infects a permissive target cell through first adhering to a dedicated target receptor. For SARS-CoV-2, the homotrimeric Spike glycoprotein (also commonly referred to as the S-antigen) expressed on infectious virions mediates binding to target cells via an interaction with the host receptor, angiotensin-converting enzyme 2 (ACE2) [50]. More specifically, the SARS-CoV-2 S-antigen possesses a stretch of amino acids in the S1 subunit that is designated the "receptor binding domain" (RBD) and which binds to ACE2 with nanomolar affinity [51]. Antibodies targeting the SARS-CoV-2 RBD can therefore disrupt the association of S-antigen with ACE2 and correlate with neutralizing activity [52,53]. When comparing the B_{mem} elicited in donors following infection or vaccination, it therefore seemed critical to further restrict the investigation of B_{mem} to those recognizing the RBD region of the WH1-S protein.

Owing to the WH1-S (RBD) construct being a shorter polypeptide relative to WH1-S (FL), as well as it being a monomer vs. the trimerized WH1-S (FL) probe, we found WH1-S (RBD) less suitable for direct coating. Even when coated using an affinity capture strategy (illustrated in Supplementary Figure S2B and with which the WH1-S (FL) and WH1-NCAP data described so far were generated) we failed to detect pristine secretory footprints after direct coating with WH1-S (RBD).. We therefore leveraged an alternative strategy referred to as the "inverted assay" (illustrated in Supplementary Figure S2D) for measuring the frequencies of WH1-S (RBD)-reactive B_{mem}-derived ASCs. In this ImmunoSpot® assay variant, the ASCs are seeded onto membranes coated with capture antibodies that are specific for an Ig class of interest. In our case, since IgG^+ ASCs were the most prevalent WH1-S-reactive B_{mem} population, assay membranes were coated with an anti-human IgG Fc-specific capture reagent. Thus, similar to pan Ig-detecting assays (illustrated in Supplementary Figure S2C),

 doi:10.20944/preprints202507.1994.v1

all IgG+ ASCs are capable of generating a secretory footprint irrespective of their antigen specificity. Following removal of the cells, the antigen of interest is then added and serves as the detection probe being selectively captured by only the secretory footprints originating from antigen-specific IgG+ ASCs. Since IgG+ ASCs with irrelevant specificity greatly outnumber the antigen-specific ones following polyclonal stimulation of PBMC, such inverted assays are ideally performed using lower cell inputs than direct assays to avoid local saturation of the capture antibodies' capacity. As shown in Figure 5, inverted ImmunoSpot® assays performed utilizing either WH1-S (FL) or WH1-S (RBD) as detection probes (performed under optimal test conditions - see below) enabled visualization of pristine secretory footprints. However, using higher cell inputs we observed suboptimal secretory footprint formation, resulting as a consequence of interference between the high density of neighboring ASCs, and/or elevated membrane staining from the recapture of WH1-S (RBD)-reactive antibody distally from the source ASCs.

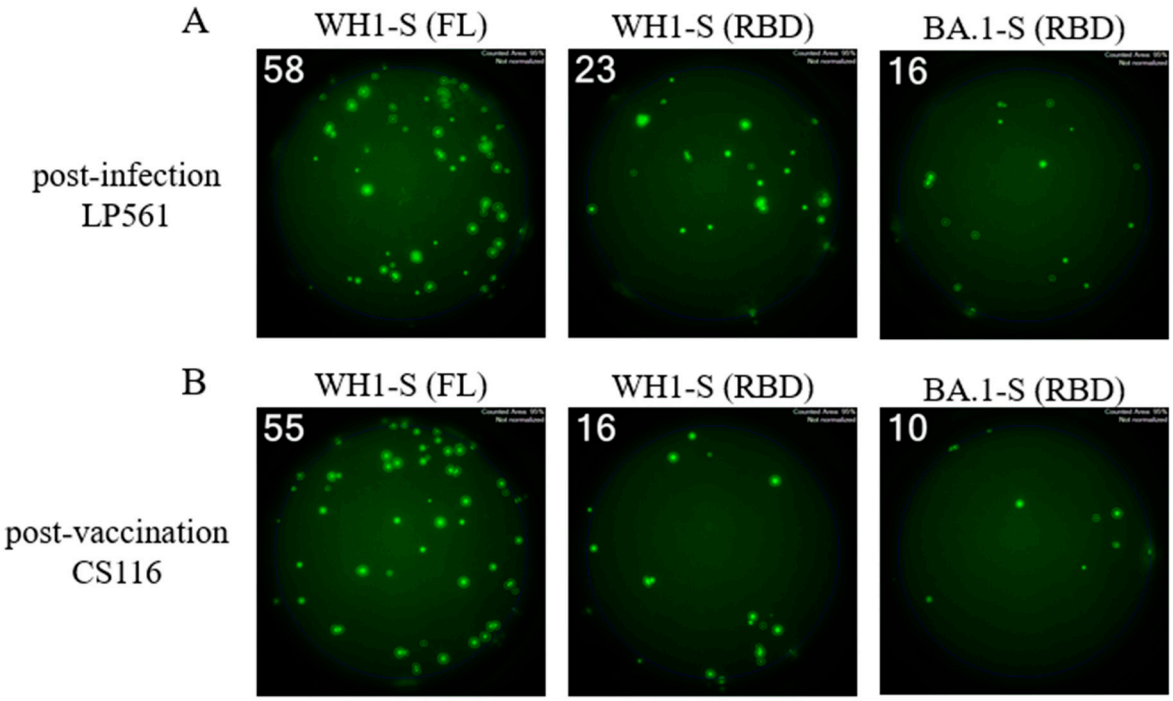

Figure 5. Single-color inverted FluoroSpot enables detection of RBD-reactive IgG+ ASCs. Representative well images from inverted assays (refer to Supplemental Figure S2D) in which polyclonally stimulated PBMC were seeded at a "Goldilocks" cell input previously determined to yield ~50 SFUs in a direct assay using affinity capture coated WH1-S (FL) protein. Results obtained using the specified probes for a post-infection donor (panel A) or a post-vaccination donor (panel B) are shown. Refer to Section 2.4.3 for additional assay details.

Similar to the direct assays described previously, inverted assays can also be peformed using a serial dilution approach to define the frequency of antigen-reactive ASCs in a test sample. When we performed WH1-S (RBD) assays in parrallel with those evaluating ASC reactivity against WH1-S (FL) (in this case, WH1-S (FL) was coated using affinity capture) during the initial assessment of donor samples, we obtained a low resolution approximation of the relative frequency of WH1-S (FL)-reactive IgG+ ASCs that recognized epitopes within the RBD. However, having established in such assays the optimal number of PBMC to be plated per well for each donor to obtain a "Goldilocks cell input" (~50 SFUs), in a follow-up experiment we next sought to more precisely determine the relative frequency of WH1-S (FL)-reactive IgG+ ASCs that recognized the RBD. To this end, 8 replicate wells were seeded with the donors' pre-determined Goldilocks cell input and WH1-S-reactive IgG+ SFUs were subsequently revealed using either the WH1-S (FL) or WH1-S (RBD) probes. Owing to the increased number of replicate wells seeded with an equivalent number of PBMC, we were able to

 doi:10.20944/preprints202507.1994.v1

calculate the percentage of WH1-S (FL)-reactive IgG+ SFUs that were specific for the WH1-S (RBD) with higher resolution using this approach. Such systematic comparisons of donors from the post-infection or post-vaccination cohorts showed that in either case ~30% the WH1-S (FL)-reactive B_{mem} repertoire targeted epitopes within the WH1-S RBD. Notably, we did not observe a significant difference beween the post-infection and post-vaccination donor cohorts (Figure 6A).

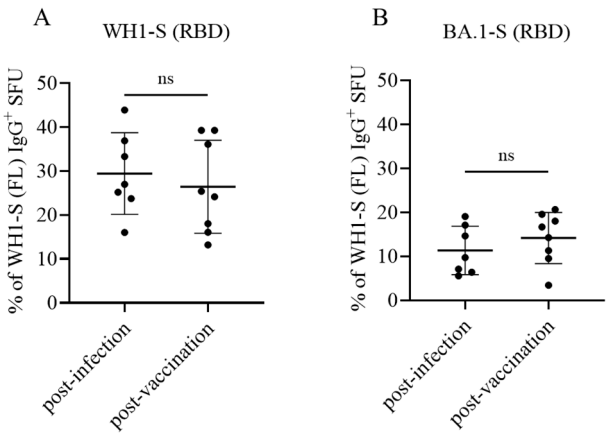

Figure 6. B_{mem} recognition of the WH1 (homotypic) or BA.1 (heterotypic) receptor binding domain (RBD). PBMC collected from SARS-CoV-2 infected (n=7) or COVID-19 mRNA vaccinated (n=8) donors were seeded into IgG-specific inverted ImmunoSpot® assays following polyclonal stimulation at donor-specific "Goldilocks" cell inputs previously determined to yield ~50 SFUs in a direct assay using affinity capture coated WH1-S (FL) protein (refer to Section 2.4.3 for additional details). Donor PBMC samples were seeded in replicate wells and the cumulative number of WH1-S (FL)-reactive SFUs detected was denoted as 100% of the donor's response. In parallel, replicate wells seeded at the same donor-specific "Goldilocks" cell input were detected using WH1-S (RBD) or BA.1-S (RBD) protein as the detection probe (see Figure 5). Percentages of WH1-S (FL)-reactive SFUs with inferred reactivity for epitopes in the WH1-S (RBD) (panel A) or BA.1-S (RBD) are denoted, respectively. Inferred frequency of WH1-S (FL)-reactive IgG+ SFUs recognizing the homotypic (WH1) or heterotypic (BA.1) RBD probes were not significantly different between the post-infection or post-vaccination cohorts by two-tailed unpaired t-tests (p=0.57 for WH1 and p=0.35 for BA.1, respectively).

Collectively, these data (namely, similar frequencies of WH1-S (FL)-reactive IgG+ B_{mem} recognizing epitopes in the RBD) suggest that the neutralizing potential of secondary recall responses in case of (re)-infection with the homotypic WH1 strain would be similar in both cohorts. This notion is critical, as several studies have shown that the concentrations and neutralizing capacity of plasma/serum antibodies declined after infection or the initial prime-boost COVID-19 vaccination regimen [54–58].

3.5. Comparing Omicron cross-reactive B_{mem} in WH1 vaccinated vs. WH1 infected individuals

New variants of a virus arise as a consequence of their ability to evade pre-existing neutralizing antibody activity elicited by the previously circulating strain(s). Next to enabling affinity maturation of antibodies directed against the homotype, somatic hypermutation also serves to increase the likelihood that clonally expanded and class-switched B_{mem} capable of recognizing future variants are also generated [26]. If such cross-reactive cells are already present within the B_{mem} repertoire, upon subsequent infection with a heterotypic virus they will enable faster, secondary-type recall antibody responses. We therefore tested to what extent the B_{mem} repertoires induced following infection or vaccination with WH1-S would cross-react with the RBD of an Omicron variant (BA.1) that emerged after these blood samples were collected [21]. Having already established for each test subject the frequency of WH1-S (RBD)-reactive B_{mem} relative to the frequency of WH1-S (FL)-reactive B_{mem} through performing inverted assays using serially diluted PBMC, as an additional component to our

 doi:10.20944/preprints202507.1994.v1

higher resolution follow-up experiment (see above), we also included additional replicate wells to reveal the number of BA.1-S (RBD) probe-reactive IgG^+ ASCs. In line with the large number of immune-evading mutations acquired within the RBD region of the BA.1 Omicron variant [59,60], we observed that both post-infection and post-vaccination samples exhibited a similarly low frequency (ranging between 5-20%) of WH1-S-reactive IgG^+ B_{mem}-derived ASCs capable of recognizing the BA.1-S (RBD) probe (Figure 6B). These data demonstrate that a comparable subset of the WH1-S-reactive IgG^+ B_{mem} generated following either infection or vaccination would be capable of recognizing epitopes maintained with the RBD region of BA.1 and therefore would have the potential to contribute towards an anamnestic host defense reaction following a breakthrough infection [61,62].

4. Summary and conclusions

Enabled by new developments in the field of B cell ImmunoSpot® analysis, we provide here a comprehensive analysis of WH-1 S-antigen-reactive B_{mem} elicited in the simplest immune scenario, in previously naïve subjects following their first infection with the original "prototype" or the original COVID-19 mRNA vaccine encoding the same WH1-S antigen. Perhaps surprisingly from the standpoint of basic immunology expectations, the B_{mem} repertoires generated in these two cohorts were found to be quite similar, although the biological significance of the subtle differences seen in IgA^+ and $IgG4^+$ B_{mem} populations is not clear. This study was restricted to sample cohorts for which defined exposure histories were available. This "first of its kind" systematic characterization of B cell memory provides basic insights into B_{mem} development under defined conditions, contrasting natural infection with vaccination. At the same time, it was intended to demonstrate the feasibility of such ImmunoSpot®-based immune monitoring for studies of more complex immunologic scenarios such as following several booster injections and/or recurrent infections with newly circulating variant strains. This report should catalyze future efforts aimed at achieving a more comprehensive assessment of antigen-specific B_{mem} in large donor cohorts (which mostly for technical reason have not been hitherto undertaken) owing to their key contributions to acquired immunity.

Supplementary Materials: The following supporting information can be downloaded at the website of this paper posted on Preprints.org.

Author Contributions: Conceptualization: G.A.K. and P.V.L.; Methodology: L.Y., N.B. and G.A.K; Formal analysis: L.Y. and G.A.K; Investigation: L.Y. and N.B.; Data curation: L.Y. and G.A.K.; Writing—original draft preparation: PVL; Writing—review and editing G.A.K., M.T.L. and P.V.L.; Supervision: G.A.K.; Project administration: G.A.K. All authors have read and agreed to the published version of the manuscript.

Funding: This research was funded by the R&D budget of Cellular Technology Limited (CTL).

Institutional Review Board Statement: PBMC samples from pre- and post-COVID-19-era donors were collected at FDA-registered collection centers from IRB-consented healthy human donors and were sold to CTL identifying donors by code only while concealing the subjects' identities. PBMC from convalescent COVID-19 donors were obtained either from the American Red Cross (Atlanta, GA, USA), BioIVT (Westbury, NY, USA), or Stem Express (Folsom, CA, USA) with IRB approval and then were sold to CTL identifying donors by code only while concealing the subjects' identities. PBMC from COVID-19 mRNA vaccinated donors were collected internally at CTL under an Advarra Approved IRB #Pro00043178 (CTL study number: GL20-16 entitled COVID-19 Immune Response Evaluation).

Informed Consent Statement: Informed consent was obtained from all subjects collected internally under an Advarra Approved IRB #Pro00043178 (CTL study number: GL20-16 entitled COVID-19 Immune Response Evaluation).

Data Availability Statement: The data generated in this study will be made available by the authors, without undue reservation, to any qualified researcher.

 doi:10.20944/preprints202507.1994.v1

Acknowledgments: We thank Drs. Graham Pawelec and Alexey Y. Karulin for their valuable discussions and comments on the manuscript. We also want to specifically thank Tibor Baki and Victoria Gaidaenko from CTL, and Melissa Sebok, Malachi Wickman, and Jennifer Penfold from the American Red Cross for their help in acquiring PBMC samples.

Conflicts of Interest: P.V.L. is Founder, President, and CEO of Cellular Technology Limited (CTL), a company that specializes in immune monitoring by ImmunoSpot®. M.T.L. is a cofounder and CSO of CTL. L.Y., N.B., and G.A.K. are employees of CTL. This study was funded by CTL, and the funder directed the study design, collection, analysis, interpretation of data, the writing of this article, and made the decision to submit it for publication.

References

1. Randall, T.D. and R.E. Mebius, *The development and function of mucosal lymphoid tissues: a balancing act with micro-organisms.* Mucosal Immunol, 2014. **7**(3): p. 455-66.
2. Bemark, M. and D. Angeletti, *Know your enemy or find your friend?-Induction of IgA at mucosal surfaces.* Immunol Rev, 2021. **303**(1): p. 83-102.
3. Giri, S., et al., *Quantity of Vaccine Poliovirus Shed Determines the Titer of the Serum Neutralizing Antibody Response in Indian Children Who Received Oral Vaccine.* J Infect Dis, 2018. **217**(9): p. 1395-1398.
4. Long, Q.X., et al., *Antibody responses to SARS-CoV-2 in patients with COVID-19.* Nat Med, 2020. **26**(6): p. 845-848.
5. Pichilingue-Reto, P., et al., *Serum IgG Profiling of Toddlers Reveals a Subgroup with Elevated Seropositive Antibodies to Viruses Correlating with Increased Vaccine and Autoantigen Responses.* J Clin Immunol, 2021. **41**(5): p. 1031-1047.
6. Vidarsson, G., G. Dekkers, and T. Rispens, *IgG subclasses and allotypes: from structure to effector functions.* Front Immunol, 2014. **5**: p. 520.
7. Duchemin, M., et al., *Antibody-Dependent Cellular Phagocytosis of HIV-1-Infected Cells Is Efficiently Triggered by IgA Targeting HIV-1 Envelope Subunit gp41.* Front Immunol, 2020. **11**: p. 1141.
8. Russell, M.W. and B. Mansa, *Complement-fixing properties of human IgA antibodies. Alternative pathway complement activation by plastic-bound, but not specific antigen-bound, IgA.* Scand J Immunol, 1989. **30**(2): p. 175-83.
9. Steffen, U., et al., *IgA subclasses have different effector functions associated with distinct glycosylation profiles.* Nat Commun, 2020. **11**(1): p. 120.
10. Hufnagl, K., et al., *Intranasal tolerance induction with polypeptides derived from 3 noncross-reactive major aeroallergens prevents allergic polysensitization in mice.* J Allergy Clin Immunol, 2005. **116**(2): p. 370-6.
11. Tsitoura, D.C., et al., *Intranasal exposure to protein antigen induces immunological tolerance mediated by functionally disabled CD4+ T cells.* J Immunol, 1999. **163**(5): p. 2592-600.
12. Unger, W.W., et al., *Nasal tolerance induces antigen-specific CD4+CD25- regulatory T cells that can transfer their regulatory capacity to naive CD4+ T cells.* Int Immunol, 2003. **15**(6): p. 731-9.
13. Tordesillas, L. and M.C. Berin, *Mechanisms of Oral Tolerance.* Clin Rev Allergy Immunol, 2018. **55**(2): p. 107-117.
14. Butcher, M.J. and J. Zhu, *Recent advances in understanding the Th1/Th2 effector choice.* Fac Rev, 2021. **10**: p. 30.
15. Duan, T., et al., *Toll-Like Receptor Signaling and Its Role in Cell-Mediated Immunity.* Front Immunol, 2022. **13**: p. 812774.
16. Forsthuber, T., H.C. Yip, and P.V. Lehmann, *Induction of TH1 and TH2 immunity in neonatal mice.* Science, 1996. **271**(5256): p. 1728-30.
17. Gottwein, J.M., et al., *Protective anti-Helicobacter immunity is induced with aluminum hydroxide or complete Freund's adjuvant by systemic immunization.* J Infect Dis, 2001. **184**(3): p. 308-14.
18. Stavnezer, J. and C.E. Schrader, *IgH chain class switch recombination: mechanism and regulation.* J Immunol, 2014. **193**(11): p. 5370-8.
19. de Taeye, S.W., et al., *FcgammaR Binding and ADCC Activity of Human IgG Allotypes.* Front Immunol, 2020. **11**: p. 740.

 doi:10.20944/preprints202507.1994.v1

20. Koenig, J.F.E., et al., *Type 2-polarized memory B cells hold allergen-specific IgE memory.* Sci Transl Med, 2024. **16**(733): p. eadi0944.
21. Viana, R., et al., *Rapid epidemic expansion of the SARS-CoV-2 Omicron variant in southern Africa.* Nature, 2022. **603**(7902): p. 679-686.
22. Berber, E. and T.M. Ross, *Factors Predicting COVID-19 Vaccine Effectiveness and Longevity of Humoral Immune Responses.* Vaccines (Basel), 2024. **12**(11).
23. Post, N., et al., *Antibody response to SARS-CoV-2 infection in humans: A systematic review.* PLoS One, 2020. **15**(12): p. e0244126.
24. Akkaya, M., K. Kwak, and S.K. Pierce, *B cell memory: building two walls of protection against pathogens.* Nat Rev Immunol, 2020. **20**(4): p. 229-238.
25. Palm, A.E. and C. Henry, *Remembrance of Things Past: Long-Term B Cell Memory After Infection and Vaccination.* Front Immunol, 2019. **10**: p. 1787.
26. Matz, H.C., K.M. McIntire, and A.H. Ellebedy, *'Persistent germinal center responses: slow-growing trees bear the best fruits'.* Curr Opin Immunol, 2023. **83**: p. 102332.
27. Kirchenbaum, G.A., G. Pawelec, and P.V. Lehmann, *The Importance of Monitoring Antigen-Specific Memory B Cells, and How ImmunoSpot Assays Are Suitable for This Task.* Cells, 2025. **14**(3).
28. Smith, S.A. and J.E. Crowe, Jr., *Use of Human Hybridoma Technology To Isolate Human Monoclonal Antibodies.* Microbiol Spectr, 2015. **3**(1): p. AID-0027-2014.
29. Boonyaratanakornkit, J. and J.J. Taylor, *Techniques to Study Antigen-Specific B Cell Responses.* Front Immunol, 2019. **10**: p. 1694.
30. Koppert, S., et al., *Affinity Tag Coating Enables Reliable Detection of Antigen-Specific B Cells in Immunospot Assays.* Cells, 2021. **10**(8).
31. Lehmann, P.V., et al., *Theoretical and practical considerations for validating antigen-specific B cell ImmunoSpot assays.* J Immunol Methods, 2025. **537**: p. 113817.
32. Becza, N., et al., *Optimizing PBMC Cryopreservation and Utilization for Immunospot® Analysis of Antigen-Specific Memory B Cells.* Vaccines, 2025. **13**(7): p. 765.
33. Yao, L., et al., *Four-Color ImmunoSpot((R)) Assays Requiring Only 1-3 mL of Blood Permit Precise Frequency Measurements of Antigen-Specific B Cells-Secreting Immunoglobulins of All Four Classes and Subclasses.* Methods Mol Biol, 2024. **2768**: p. 251-272.
34. Pinna, D., et al., *Clonal dissection of the human memory B-cell repertoire following infection and vaccination.* Eur J Immunol, 2009. **39**(5): p. 1260-70.
35. Hsieh, C.L., et al., *Structure-based design of prefusion-stabilized SARS-CoV-2 spikes.* Science, 2020. **369**(6510): p. 1501-1505.
36. Resources, B., *Vector pCAGGS Containing the SARS-Related Coronavirus 2, Wuhan-Hu-1 Spike Glycoprotein Receptor Binding Domain (RBD), NR-52309.*
37. Karulin, A.Y., et al., *Artificial Intelligence-Based Counting Algorithm Enables Accurate and Detailed Analysis of the Broad Spectrum of Spot Morphologies Observed in Antigen-Specific B-Cell ELISPOT and FluoroSpot Assays.* Methods Mol Biol, 2024. **2768**: p. 59-85.
38. Gaunt, E.R., et al., *Epidemiology and clinical presentations of the four human coronaviruses 229E, HKU1, NL63, and OC43 detected over 3 years using a novel multiplex real-time PCR method.* J Clin Microbiol, 2010. **48**(8): p. 2940-7.
39. Wolf, C., et al., *Antibody Levels Poorly Reflect on the Frequency of Memory B Cells Generated following SARS-CoV-2, Seasonal Influenza, or EBV Infection.* Cells, 2022. **11**(22).
40. Holshue, M.L., et al., *First Case of 2019 Novel Coronavirus in the United States.* N Engl J Med, 2020. **382**(10): p. 929-936.
41. Vettermann, C. and M.S. Schlissel, *Allelic exclusion of immunoglobulin genes: models and mechanisms.* Immunol Rev, 2010. **237**(1): p. 22-42.
42. Rispens, T. and M.G. Huijbers, *The unique properties of IgG4 and its roles in health and disease.* Nat Rev Immunol, 2023. **23**(11): p. 763-778.
43. Uversky, V.N., et al., *IgG4 Antibodies Induced by Repeated Vaccination May Generate Immune Tolerance to the SARS-CoV-2 Spike Protein.* Vaccines (Basel), 2023. **11**(5).

 doi:10.20944/preprints202507.1994.v1

44. Aurelia, L.C., et al., *Increased SARS-CoV-2 IgG4 has variable consequences dependent upon Fc function, Fc receptor polymorphism, and viral variant.* Sci Adv, 2025. **11**(9): p. eads1482.
45. Gelderloos, A.T., et al., *Repeated COVID-19 mRNA vaccination results in IgG4 class switching and decreased NK cell activation by S1-specific antibodies in older adults.* Immun Ageing, 2024. **21**(1): p. 63.
46. Martin Perez, C., et al., *Post-vaccination IgG4 and IgG2 class switch associates with increased risk of SARS-CoV-2 infections.* J Infect, 2025. **90**(4): p. 106473.
47. Murin, C.D., I.A. Wilson, and A.B. Ward, *Antibody responses to viral infections: a structural perspective across three different enveloped viruses.* Nat Microbiol, 2019. **4**(5): p. 734-747.
48. Pantaleo, G., et al., *Antibodies to combat viral infections: development strategies and progress.* Nat Rev Drug Discov, 2022. **21**(9): p. 676-696.
49. Morales-Nunez, J.J., et al., *Overview of Neutralizing Antibodies and Their Potential in COVID-19.* Vaccines (Basel), 2021. **9**(12).
50. Lan, J., et al., *Structure of the SARS-CoV-2 spike receptor-binding domain bound to the ACE2 receptor.* Nature, 2020. **581**(7807): p. 215-220.
51. Walls, A.C., et al., *Structure, Function, and Antigenicity of the SARS-CoV-2 Spike Glycoprotein.* Cell, 2020. **181**(2): p. 281-292 e6.
52. Farrell, A.G., et al., *Receptor-Binding Domain (RBD) Antibodies Contribute More to SARS-CoV-2 Neutralization When Target Cells Express High Levels of ACE2.* Viruses, 2022. **14**(9).
53. Suthar, M.S., et al., *Rapid Generation of Neutralizing Antibody Responses in COVID-19 Patients.* Cell Rep Med, 2020. **1**(3): p. 100040.
54. Ferrari, D., et al., *Evaluation of antibody titer kinetics and SARS-CoV-2 infections in a large cohort of healthcare professionals ten months after administration of the BNT162b2 vaccine.* J Immunol Methods, 2022. **506**: p. 113293.
55. Jo, D.H., et al., *Rapidly Declining SARS-CoV-2 Antibody Titers within 4 Months after BNT162b2 Vaccination.* Vaccines (Basel), 2021. **9**(10).
56. Levin, E.G., et al., *Waning Immune Humoral Response to BNT162b2 Covid-19 Vaccine over 6 Months.* N Engl J Med, 2021. **385**(24): p. e84.
57. Seow, J., et al., *Longitudinal observation and decline of neutralizing antibody responses in the three months following SARS-CoV-2 infection in humans.* Nat Microbiol, 2020. **5**(12): p. 1598-1607.
58. Xiang, T., et al., *Declining Levels of Neutralizing Antibodies Against SARS-CoV-2 in Convalescent COVID-19 Patients One Year Post Symptom Onset.* Front Immunol, 2021. **12**: p. 708523.
59. Evans, J.P., et al., *Neutralization of SARS-CoV-2 Omicron sub-lineages BA.1, BA.1.1, and BA.2.* Cell Host Microbe, 2022. **30**(8): p. 1093-1102 e3.
60. Kumar, S., K. Karuppanan, and G. Subramaniam, *Omicron (BA.1) and sub-variants (BA.1.1, BA.2, and BA.3) of SARS-CoV-2 spike infectivity and pathogenicity: A comparative sequence and structural-based computational assessment.* J Med Virol, 2022. **94**(10): p. 4780-4791.
61. Kaku, C.I., et al., *Recall of preexisting cross-reactive B cell memory after Omicron BA.1 breakthrough infection.* Sci Immunol, 2022. **7**(73): p. eabq3511.
62. Quandt, J., et al., *Omicron BA.1 breakthrough infection drives cross-variant neutralization and memory B cell formation against conserved epitopes.* Sci Immunol, 2022. **7**(75): p. eabq2427.